Striation and plasma bullet propagation in an atmospheric pressure plasma jet

Sun Ja Kim, T. H. Chung,[a] and S. H. Bae
Department of Physics, Dong-A University, Busan 604-714, Republic of Korea

(Received 15 December 2009; accepted 29 March 2010; published online 7 May 2010)

An atmospheric pressure plasma jet source driven by pulsed wave of several tens of kilohertz and by sinusoidal wave was designed and characterized. A newly designed jet consists of a sharpened tungsten pin electrode covered with a cone type Teflon layer confined in a Pyrex tube. This structure provides an efficient ignition since the electric field is concentrated on the end of electrode. Using the electrical and optical characterization, the properties of plasma bullet were explored. For the Ar plasma jet driven by a pulsed wave at low duty cycles, the volume, the speed, and the luminosity of the plasma bullet became larger, and the striation behavior was observed. © *2010 American Institute of Physics*. [doi:10.1063/1.3400220]

I. INTRODUCTION

Atmospheric pressure plasma jet and its applications for material processing and biomedical treatment have recently become hot issues of nonthermal plasma research.[1,2] It has been operated at an excitation frequency either in several tens of kilohertz ac range (or pulsed mode) or in radio-frequency (rf) range.[3–5] Various kinds of nonthermal plasma jet have distinct characteristics and the efficiency of the treatment depends on the essential parameters of the plasma.[6,7] However, distinct mechanisms responsible for the production of atmospheric pressure plasma jet have not been verified. It was found that the plasma jet is constituted of discrete bulletlike plasma clouds moving at a velocity much higher than the gas velocity. Recent reports proposed discharge models to explain the properties of plasma bullets.[8–10] Further experimental investigations are needed to advance the understanding of atmospheric pressure plasma jet. In this work, the electrical and optical properties of a specially designed plasma jet driven by several tens kilohertz of pulsed dc and ac (or rf) wave are reported. The propagation of plasma bullets and the striation behavior are also investigated.

II. EXPERIMENTAL SETUP

Figure 1 shows the jet source driven by pulsed dc voltage with repetition rates of several tens of kilohertz (or several tens of kilohertz ac voltage). At the center of the Pyrex tube is a tungsten wire with a diameter of 0.6 mm and a pencil-shaped tapered end. The wire is concentric with a Pyrex tube, which has an inside diameter of 10 mm and an outside diameter of 12 mm. The Pyrex tube is covered with a stainless steel holder (14 mm inner diameter, 18 mm outer diameter). This source can generate plasma jet in many different gases and using different electrical excitations. The power sources (FTLab HPSI200 or PDS 4000) of several tens of kilohertz wave (or pulse) are applied to the tungsten wire. Another rf power source (YS E03F) of 13.56 MHz can be applied to the wire through a matching network. The wire shaft is covered with a cone-type Teflon layer tube, leaving a length of 10 mm of the wire exposed to gas. The diameter of the Pyrex tube nozzle is 2 mm. The tip-to-nozzle distance is 10 mm. The Pyrex tube is filled with argon gas fed through the six holes (1.5 mm diameter) in the Teflon tube. The electric field near the wire and at the gas flow layer was calculated using an electrostatic model provided by CFD-ACE+.[11] Figure 2(a) shows the two-dimensional distribution of electric field strength without plasma generation. Figure 2(b) represents the geometry of the wire and surrounding cone-type dielectrics with gas-flowing holes (top), and the electric field strength near the wire and at the gas flow layer along the wire axis (bottom). This structure provides an efficient ignition since the electric field is concentrated near the end of the pin (wire) electrode. The electric field has the components both perpendicular and parallel to the wire axis. The argon gas was delivered at a flow rate in the range of 0.5–3 l/min, controlled by a flow meter (Kofloc RK1600R). The electrical properties of the discharge were studied by simultaneous measurement of the voltage and current across the discharge. The measurements were done by using a high voltage probe (Tektronix P5100) and a current probe (Pearson 3972). The results were recorded on a real time digital oscilloscope (LeCroy WS44XS-A). To image the plume of plasma jet on a nanosecond scale, an intensified charge coupled device (ICCD) camera (PI-MAX2, Princeton Instrument) was used with its triggering achieved using a pulse generator.

III. RESULTS AND DISCUSSION

Figure 3(a) shows the voltage-current characteristics of the pulsed discharge. The pulsed source delivered a unipolar pulse train having a peak voltage of 2.5 kV. The pulse width was fixed at 10 μs at a duty cycle of 47%. The figure show two narrow current pulses with a short duration, a positive one as the voltage increased and a negative one as the voltage decreased. Lu and Laroussi[8] have shown that for a pulsed dielectric barrier discharge (DBD) jet operated at atmospheric pressure, two discharges are ignited per pulse.

[a]Author to whom correspondence should be addressed. Electronic mail: thchung@dau.ac.kr.

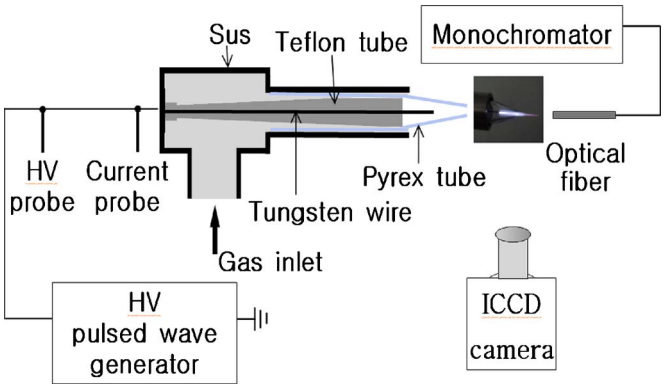

FIG. 1. (Color online) Schematic of the experimental setup.

Our corona-DBD hybrid discharge system exhibits a similar property to that of DBD jet. The discharge due to the negative current pulse was much weaker than the first discharge (due to the positive current pulse) and extinguished fast (as will be shown later). The negative current pulse is caused by the voltage induced by the charge accumulation on the dielectric tube during the first current pulse.[8] Figure 3(b) shows the voltage-current characteristics of the sinusoidal driven source with a peak-to-peak voltage of 2.72 kV at an excitation frequency of 50 kHz.

Figure 4(a) shows the captured photographs of the plasma bullet taken at different delay time using ICCD camera. The exposure time of the ICCD camera was 20 ns. The applied voltage, excitation frequency, duty cycle, and gas flow rate were 1.8 kV, 50 kHz, 47%, and 1 l/min, respectively. The sequent images were taken at the region near the pin electrode at every 100 ns. The number of accumulation time was 3000 for the gate mode. It is observed that the plasma plume is a propagation of bullets rather than a continuous volume of plasma. The propagation velocity of plasma bullet is estimated to be from 0.9×10^4 to 2×10^4 m/s with increasing applied voltage. Lu and Laroussi[8] proposed a streamer discharge model based on photon ionization to explain the dynamics of the plasma plume. This model of self-sustaining streamers was developed by Dawson and Winn.[12] A special form of gas breakdown is generated in the case of a needle-shaped electrode that produces a nonuniform electric field, and then the ionization wave propagates in the form of a streamer. The charge distribution in the streamer strengthens the electric field near its head. Ionization processes occur with excitations of atoms or molecules. Photons generated by radiation from excited particles are absorbed in neighboring regions,

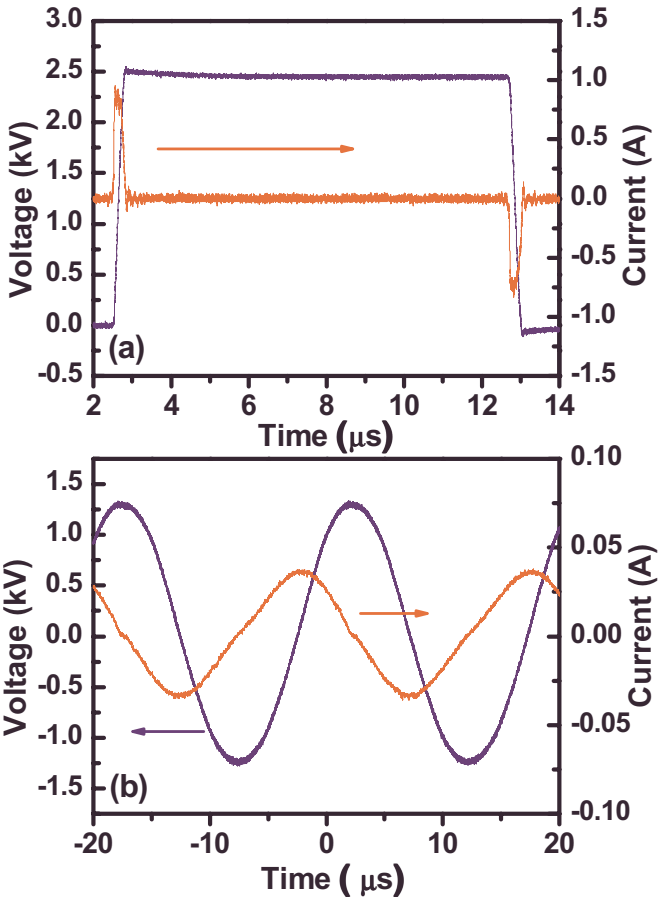

FIG. 3. (Color online) Waveforms of the total current and the applied voltage for different discharge conditions, (a) pulsed and (b) sinusoidal excitation. The gas flow rate was 0.5 l/min.

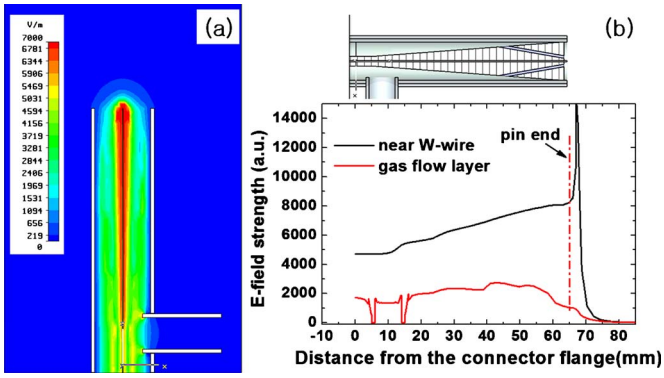

FIG. 2. (Color online) (a) Two-dimensional distribution of electric field strength before the plasma generation. (b) The geometry of the wire and surrounding cone-type dielectrics with holes (top), the electric field strength along the wire axis (bottom). The dotted line indicates the position of the pin end.

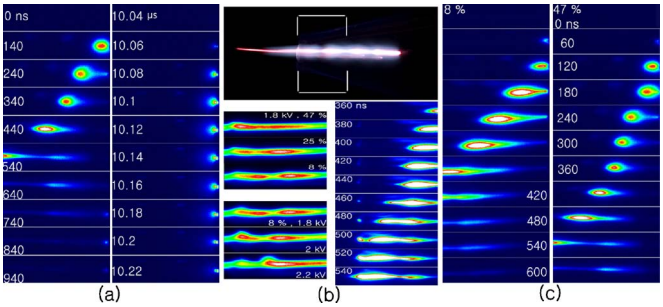

FIG. 4. (Color online) (a) ICCD images of the plasma bullet taken at different delay time under the gate mode (at duty cycle 47%). (b) The overall view of the jet plasma showing the striation behavior at 1.8 kV and 8% (top), the images of plasma plume under the shutter mode (bottom left), and the sequent images of plasma bullet taken at the region represented by the rectangle in the top figure (bottom right). (c) Comparison of the sequent images at duty cycles 8% and 47%.

and the absorption of photons can lead to ionization and the creation of free electrons. The intensity of this ionization process is weak, but the appearance of free electrons in the region of high electric field leads to their rapid reproduction. The head of the streamer propagates to a new position following the direction of the electric field.[13] The track left by the plasma bullet was observed to be dark but not negligible under most conditions.[9] The image at 740 ns shows the secondary discharge due to the connecting channel of electrode and conductivity of the dark track left by the bullet. This observation is quite consistent with the previous study.[8] During the voltage-falling phase (at 10 μs), aforementioned weak discharge due to the negative current pulse is observed but noticeable bullet propagation is not shown [the right column of Fig. 4(a)]. In an ac driven plasma jet, plasma bullets tend to form in the positive half cycle which produces positive current pulse.[14]

The ionization wave velocity due to electron diffusion can be expressed as $v=2[\upsilon_i D_a]^{1/2}$, where υ_i is the ionization frequency and D_a is the ambipolar diffusion coefficient.[10,15] For a nonequilibrium plasma, D_a is expressed as $D_a=\mu_+(k_B T_e/e)$, where μ_+ is the ion mobility and k_B is the Boltzmann constant. In the case of ions in argon, $\mu_+ \doteqdot 1.315$ cm^2/V s.[16] The frequency of Ar ionization by electrons is estimated to be about 3.6×10^{11}/s (Ref. 10) and the electron temperature (T_e) is estimated to be 0.4 eV from the modified Boltzmann plot method utilizing the Ar $4p\rightarrow4s$ optical transitions.[17] With these parameters, the velocity of the ionization wave is estimated to be about 8.7×10^3 m/s. In the study of Hong *et al.*[18] on a nitrogen plasma jet, much larger value of μ_+ and much smaller value of υ_i were used compared to those in this work. Their estimation was based on the drift velocity and the ionization coefficient $\alpha=p\ f(E/p)$ where E is the electric field and p is pressure. As mentioned earlier, the propagation velocity of plasma bullet is estimated to be about 9×10^3 m/s and it is close to the estimated ionization wave velocity. Therefore, it is possible to state that plasma bullet is produced by cathode-oriented ionization wave front.

Figure 4(b) shows the picture of the discharge and the plasma plume (top), ICCD images under the shutter mode (left) both showing the striation behavior, and the sequent images under the gate mode (right). In the top figure, the pin electrode is located to the right edge of the jet plasma and the plume is emanating to the left (into environment) through the nozzle. The bottom figures were taken at the region represented by the rectangle in the top figure. The left figures represent three cases of the duty cycles, 47%, 25%, and 8% (at 1.8 kV) and of the applied voltage 1.8, 2.0, and 2.2 kV (at duty cycle 8%). At low duty cycles (most typically 8% here), the striation behavior was observed (top figure). The distance between the bright nodes was about 1.4 mm. The striation of plasma plume becomes significant as the plasma duty cycle decreases and the applied voltage increases. The striations are related to positive space charge wave generated by the self-sustained perturbations that originate from the force balance between the ion and the electron wall-charge clouds accumulated on the dielectric layer.

To investigate detailed behavior, the plasma bullet was observed near the pin electrode in two cases of the duty cycle 47% and 8% with other parameters unchanged. Figure 4(c) shows that at the duty cycle of 8%, the plasma ignition is easier, and the volume and luminosity and velocity of plasma bullet increase. This indicates that the charges accumulated on the dielectric layer have more significant effect on the bullet in the case of low duty cycle. The applied voltage, the duty cycle, and the distance between dielectric layer and electrode, altogether, influence the properties of plasma bullet and the striation behavior. Among them the effect of duty cycle is most significant on the formation of striation. In a pulsed discharge, the electron temperature drops to very small values after the power is turned off. However, the peak electron temperature in a transient process becomes higher at a lower duty cycle. The peak electron density increases as the duty cycle decreases, which is due to an increase in T_e associated with higher power during the discharge on time.[19] More importantly, shorter pulse width allows for the use of much elevated applied voltage to induce larger peak discharge current (hence higher electron density), both desirable for active plasma chemistry.[20] Enhanced electron density and electron temperature explains the larger volume and luminosity of the bullet at the duty cycle of 8%. In addition, as the pulse width decreases, the interval between the primary discharge (due to the positive current peak) and the weak discharge (due to the negative current peak) is shortened, and the nonuniform electric field gradient becomes strong. All these factors enhance the perturbation and cause the density modulation with patterns of bellies and nodes. The striation behavior may be caused by the change in local electric field in the tube. As can be seen from the figure, when the striation occurs, the bullet itself has a larger shape and higher luminosity, which is caused by the ponderomotive force due to a strong electric field gradient along the tube axis. The ponderomotive force can be formulated as $\mathbf{F}_p=-\omega_p^2/\omega^2\nabla\langle\varepsilon_0 E^2/2\rangle$ (ω_p, ω, and ε_0 are the plasma frequency, the driving frequency, and the permittivity of vacuum, respectively).[21] The electric field E consists of the transient electric field imposed by external voltage pulses and the field formed between the propagating ionization front and the charge-accumulated dielectric surface. As shown in Fig. 2, this device has a large gradient of the electric field. Also, the electron density becomes high when the duty cycles are low. All these factors contribute to the formation of the striation inside the Pyrex tube by increasing the ponderomotive force. However, the striation did not appear outside of a nozzle.

Optical spectra were recorded for emission along the axis of the plasma jet (detected at the distance of 0.5 cm from the nozzle) in the range from 200 to 900 nm. The emitted light was focused by means of optical fiber into entrance slit of 0.75 m monochromator (SPEX 1702), equipped with a grating of 1200 grooves per millimeter and slit width of 100 μm. Figure 5 shows the emission spectra observed in the plasma plume. The different spectra of Ar plasma jet driven by (a) pulsed source, (b) sinusoidal source, and (c) rf source were compared. The spectra clearly indicate that excited O, OH, N_2, N_2^+, and Ar exist in the plasma plume. Stronger excited N_2^+ emission was observed for the pulsed

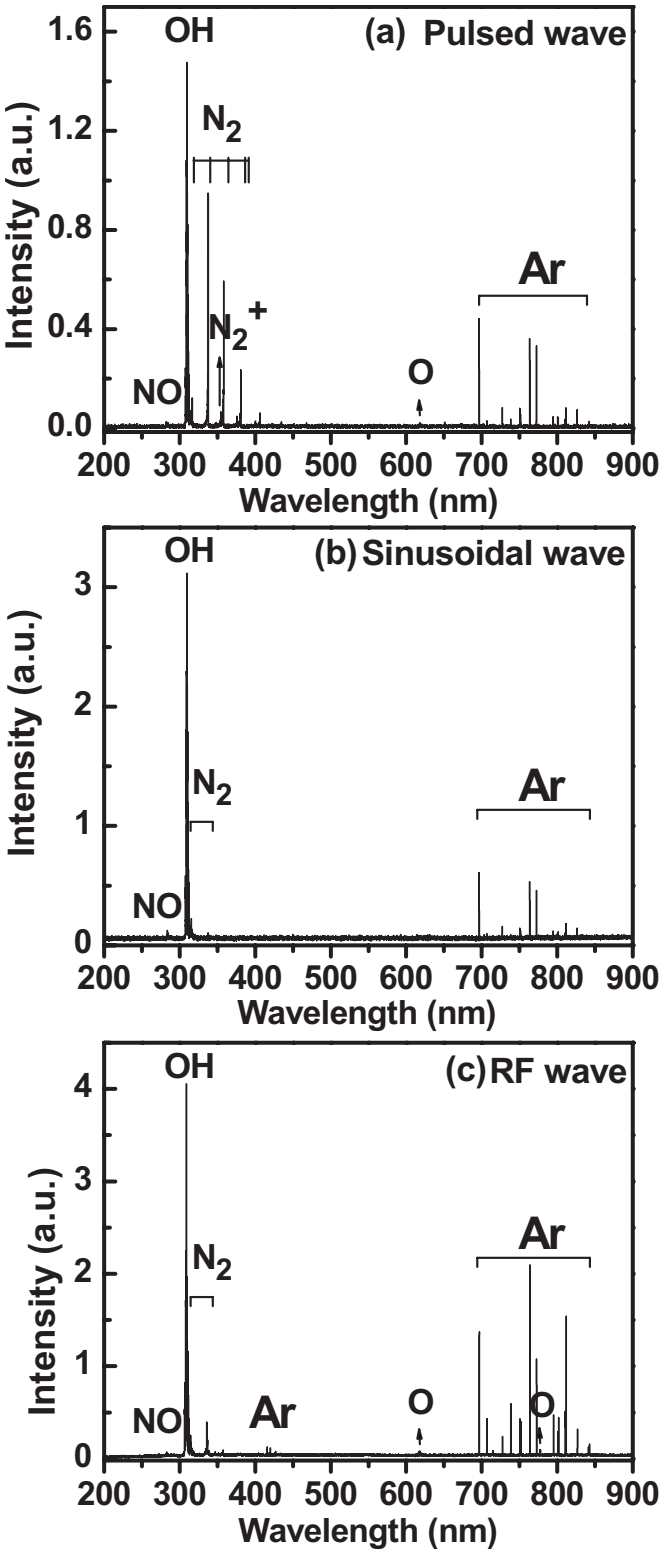

FIG. 5. Optical emission spectra from 200 to 900 nm observed in (a) pulse-driven (1.9 kV, duty cycle 25%), (b) sinusoidal-driven source (V_{rms}=1.2 kV), and (c) rf-driven source (7 W). The gas flow rate was 0.5 l/min.

plasma jet than the sinusoidal wave jet. Highly reactive radicals such as OH enhanced compared to other excited species. The rf plasma jet spectrum has much higher intensity and more argon atomic lines indicating larger plasma density and/or electron temperature. The pulsed discharge maintains

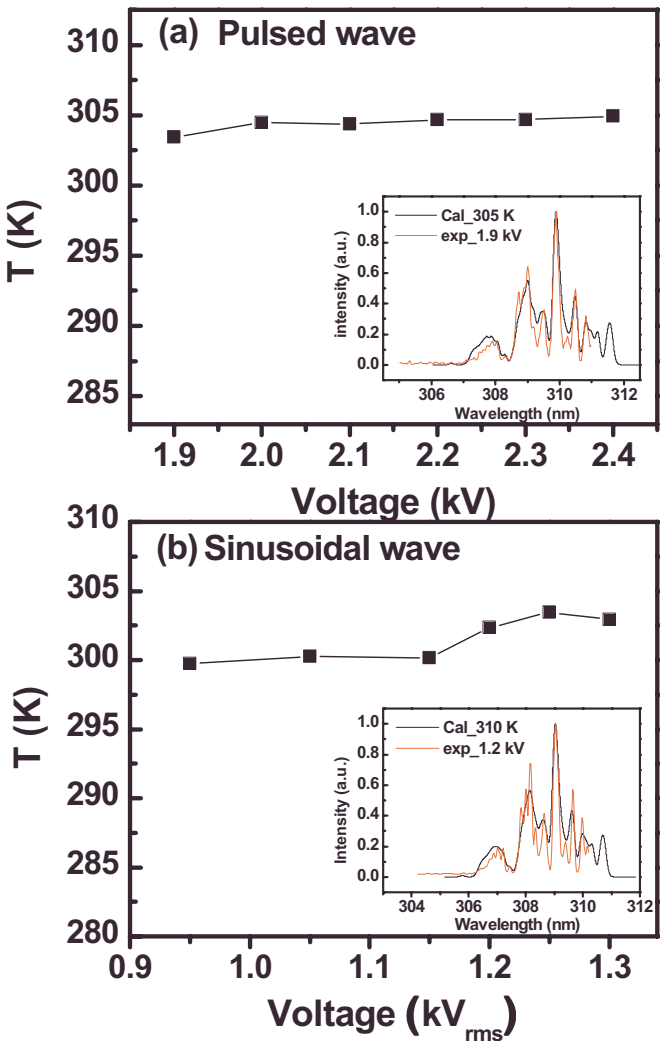

FIG. 6. (Color online) Comparison of the measured and simulated gas temperature as a function of applied voltage for (a) the pulsed source and (b) the sinusoidal source. The gas flow rate was 0.5 l/min.

a comparable level of the emission intensity to those of the rf discharge. This indicates that a low-frequency pulsed operation of the plasma jet can provide sufficient amount of radicals without the gas temperature rise.

Figure 6 shows the gas temperature measured by using a fiber optic temperature sensor (Luxtron, M601-DM&STF) as a function of applied voltage for (a) the pulsed source and (b) the sinusoidal source. The gas flow rate was kept constant at 0.5 l/min. It is observed that the gas temperature is as low as the room temperature. The gas temperature (T_g) of the plasma can be also deduced from the rotational temperature (T_r) of diatomic species, which is expected to be in equilibrium with T_g. The rotational temperature of a molecule can be obtained by comparing the synthetic diatomic molecular spectrum with measured one.[22] To obtain the best fit between the experimental and the synthetic spectral bands, a least-square procedure was used. A typical fitting of the measured band spectrum with the synthetic spectrum is shown in the inset. The OH band ($A\ ^2\Sigma^+ \rightarrow X\ ^2\Pi$ transition) from 306 and 310 nm was fitted to obtain OH rotational temperature. Good

agreement between the measured spectrum and the synthetic one suggests reasonable evaluation of T_r.

IV. CONCLUSION

In this work, a newly designed atmospheric pressure plasma jet device with a cone-type dielectric layer exhibits plasma stability while maintaining efficient reaction chemistry and room temperature in broad operating conditions. The bullet propagation is mainly dependent on the applied voltage and the duty cycle. For the Ar plasma jet driven by a pulsed wave at low duty cycle of 8%, the volume and the luminosity of the plasma bullet became larger compared to those at duty cycles of 25% and 47%. The plasma bullet propagated faster at low duty cycles. A strong electric field associated with a short pulse width imposed on the large electric field gradient inherent to the device gives rise to the ponderomotive force. The fact that a striation behavior is observed at low duty cycles indicates that it can be attributed the ponderomotive force.

ACKNOWLEDGMENTS

Helpful discussions with Mr. Chang-Seung Ha, Professor Ho-Jun Lee, and Professor Hae June Lee of Pusan National University are greatly acknowledged. This work was supported by the Korea Science and Engineering Foundation under Contract No. 2009-0067223.

[1] M. Laroussi and T. Akan, Plasma Processes Polym. **4**, 777 (2007).
[2] R. E. J. Sladek and E. Stoffels, J. Phys. D: Appl. Phys. **38**, 1716 (2005).
[3] X. Lu, Z. Jiang, Q. Xiong, Z. Tang, X. Hu, and Y. Pan, Appl. Phys. Lett. **92**, 081502 (2008).
[4] G. Li, H.-P. Li, L.-Y. Wang, S. Wang, H.-X. Zhao, W.-T. Sun, X.-H. Xing, and C.-Y. Bao, Appl. Phys. Lett. **92**, 221504 (2008).
[5] C.-S. Ha, J. Y. Choi, D. H. Kim, C. H. Park, H. J. Lee, and H. J. Lee, Appl. Phys. Lett. **95**, 061502 (2009).
[6] S. Perni, G. Shama, J. L. Hobman, P. A. Lund, C. J. Kershaw, G. A. Hidalgo-Arroyo, C. W. Penn, X. T. Deng, J. L. Walsh, and M. G. Kong, Appl. Phys. Lett. **90**, 073902 (2007).
[7] S. J. Kim, T. H. Chung, and S. H. Bae, Appl. Phys. Lett. **94**, 141502 (2009).
[8] X. Lu and M. Laroussi, J. Appl. Phys. **100**, 063302 (2006).
[9] X. Lu, Q. Xing, J. Hu, F. Zhou, W. Gong, Y. Xian, C. Zou, Z. Tang, Z. Jiang, and Y. Pan, J. Appl. Phys. **105**, 043304 (2009).
[10] J. Shi, F. Zhong, J. Zhang, D. W. Liu, and M. G. Kong, Phys. Plasmas **15**, 013504 (2008).
[11] See http://www.cfdrc.com/ for CFD-ACE+ code, CFD Research Corporation.
[12] G. A. Dawson and W. P. Winn, Z. Phys. **183**, 159 (1965).
[13] B. M. Smirnov, *Physics of Ionized Gases* (Wiley, Canada, 2001).
[14] J. L. Walsh, F. Iza, N. B. Janson, V. J. Law, and M. G. Kong, J. Phys. D: Appl. Phys. **43**, 075201 (2010).
[15] A. Böhle, O. Ivanov, A. Kolisko, U. Kortshagen, H. Schluter, and A. Vikharev, J. Phys. D: Appl. Phys. **29**, 369 (1996).
[16] A. L. Ward, J. Appl. Phys. **33**, 2789 (1962).
[17] F. J. Gordillo-Vázquez, M. Camero, and C. Gomez-Aleixandre, Plasma Sources Sci. Technol. **15**, 42 (2006).
[18] Y. C. Hong, H. S. Uhm, and W. J. Yi, Appl. Phys. Lett. **93**, 051504 (2008).
[19] S. Ashida, C. Lee, and M. A. Lieberman, J. Vac. Sci. Technol. A **13**, 2498 (1995).
[20] J. L. Walsh, D. X. Liu, F. Iza, M. Z. Rong, and M. G. Kong, J. Phys. D: Appl. Phys. **43**, 032001 (2010).
[21] F. F. Chen, *Introduction to Plasma Physics and Controlled Fusion* (Plenum, New York, London, 1984).
[22] S. Y. Moon and W. Choe, Spectrochim. Acta, Part B **58**, 249 (2003).